

X-ray Pulsations from the Central Source in Puppis A

G. G. Pavlov

The Pennsylvania State University, 525 Davey Lab, University Park, PA 16802, USA;
 pavlov@astro.psu.edu

and

V. E. Zavlin and J. Trümper

Max-Planck-Institut für extraterrestrische Physik, D-85740 Garching, Germany;
 zavlin@xray.mpe.mpg.de

ABSTRACT

There are several supernova remnants which contain unresolved X-ray sources close to their centers, presumably radio-quiet neutron stars. To prove that these objects are indeed neutron stars, to understand the origin of their X-ray radiation, and to explain why they are radio-quiet, one should know their periods and period derivatives. We searched for pulsations of the X-ray flux from the radio-quiet neutron star candidate RX J0822–4300 near the center of the Puppis A supernova remnant observed with the *ROSAT* PSPC and HRI. A standard timing analysis of the separate PSPC and HRI data sets does not allow one to detect the periodicity unequivocally. However, a thorough analysis of the two observations separated by 4.56 yr enabled us to find a statistically significant period $P \simeq 75.3$ ms and its derivative $\dot{P} \simeq 1.49 \times 10^{-13}$ s s $^{-1}$. The corresponding characteristic parameters of the neutron star, age $\tau = P/(2\dot{P}) = 8.0$ kyr, magnetic field $B = 3.4 \times 10^{12}$ G, and rotational energy loss $\dot{E} = 1.4 \times 10^{37}$ erg s $^{-1}$, are typical for young radio pulsars. Since the X-ray radiation has a thermal-like spectrum, its pulsations may be due to a nonuniform temperature distribution over the neutron star surface caused by anisotropy of the heat conduction in the strongly magnetized crust.

Subject headings: pulsars: individual (RX J0822–4300) – stars: neutron – supernovae: individual (Puppis A) – X-rays: stars

1. Introduction

Observations with the *Einstein*, *ROSAT* and *ASCA* missions have revealed several isolated, radio-quiet neutron star (NS) candidates in supernova remnants (see Brazier & Johnston 1998, for a recent review). These objects are characterized by a lack of observable radio emission,

thermal-like X-ray spectra with typical (blackbody) temperatures of $\sim (1 - 5) \times 10^6$ K, and very high ratios, $\gtrsim 1000$, of the X-ray to optical fluxes. Their X-ray radiation has been interpreted as thermal radiation from cooling NSs. The reason for the lack of observable radio emission remains unclear. The simplest explanation is that these NSs are ordinary radio pulsars whose rotational and magnetic axes are unfavorably oriented so that the pulsar beam cannot be seen at Earth. An alternative explanation is that these objects are not active radio pulsars due to, e.g., too low magnetic fields or too slow rotation. Another option is that these NSs belong to the class of anomalous X-ray pulsars, also radio-quiet, slowly rotating NSs which apparently have superstrong, $\sim 10^{14}\text{--}10^{15}$ G, magnetic fields (see, e.g., Vasisht & Gotthelf 1997). To choose among these hypotheses, one should know the rotation period and its derivative, which would allow one to estimate the object's age and magnetic field. However, many attempts to find periods in the X-ray radiation of these sources have been unsuccessful so far, which indicates that the pulsed fraction may be too low to distinguish between a signature of the true periodicity and a noise fluctuation in a relatively short observation with a small number of photons collected. On the other hand, increasing the observational time strongly increases the number of trial periods (and period derivatives in the case of very long observations). This not only makes the search prohibitively expensive, but also increases the probability of obtaining large noise fluctuations, which hampers detecting the true periodicity. However, if two or more timing observations of a source have been carried out, well separated in time, with good time resolution and sufficient amounts of photons collected, one may use additional constraints to discriminate between true and false periodicity signatures in the separate timing data. We applied such an approach to searching for periodicity of the X-ray brightest, radio-quiet NS candidate RX J0822–4300 in the supernova remnant (SNR) Puppis A, making use of *ROSAT* PSPC and HRI observations.

Puppis A is one of three known oxygen-rich SNRs in the Galaxy. Its kinematic age, 3.7 ± 0.4 kyr, was estimated from the proper motion of fast-moving filaments in the northeast quadrant of the SNR (Winkler et al. 1988). Its distance, $d = 2.2 \pm 0.3$ kpc, was estimated from VLA observations in the $\lambda 21$ cm hydrogen line in the direction of Puppis A (Reynoso et al. 1995). The central compact source was seen in the *Einstein* HRI images, located $\simeq 6'$ from the kinematical center of SNR expansion (Petre et al. 1982). Petre, Becker & Winkler (1996; hereafter PBW96) analyzed *ROSAT* HRI and PSPC observations (exposure times 4 ks and 6 ks, respectively) and suggested that this source is an isolated NS born in the supernova explosion. It has no optical counterpart to limiting magnitudes $B \gtrsim 25.0$, $R \gtrsim 23.6$, which implies an X-ray/optical flux ratio $f_X/f_B \gtrsim 5000$. No obvious radio counterpart was detected to a 3σ upper limit of 0.75 mJy at 1.4 GHz. Fitting the PSPC spectrum of the source with the blackbody model gives a temperature of 0.28 ± 0.10 keV, somewhat higher than 0.10 – 0.18 keV expected from standard NS cooling models. The corresponding blackbody radius of ~ 2 km is smaller than the expected radius for a NS. No evidence for pulsations with a pulsed fraction larger than 20% was found.

New observations of Puppis A and its central source with the *ROSAT* and *ASCA* have been performed recently. We used these data for further investigations of the spectrum and the

light curve of the NS candidate. Results of the spectral investigation will be published elsewhere (Zavlin, Pavlov, & Trümper 1998b). Briefly, they show that the temperature and radius of the NS are compatible with standard models if to assume that the NS surface is covered with a hydrogen/helium atmosphere (cf. Zavlin, Pavlov, & Trümper 1998a). Fitting the observed spectra with the NS atmosphere models indicates that the surface magnetic field may be rather high, $\gtrsim 4 \times 10^{12}$ G, so that one can expect that the NS magnetic poles are hotter than the equator (Greenstein & Hartke 1983), which may lead to observable modulation of the thermal X-ray flux.

2. Observational Data and Timing Analysis

Among several observations of Puppis A in the public archive at HEASARC/GSFC, two are suitable for searching for periodicity of the central source. The first one was carried out with the *ROSAT* PSPC on 1991 April 16 (6.0 ks useful exposure, 53 ks total time span between the beginning and the end of the observation). In that observation the NS was off-set by $\simeq 12.5''$. The background-subtracted count rate is 0.237 ± 0.006 s $^{-1}$ (0.296 ± 0.007 s $^{-1}$ after applying the dead-time and vignetting corrections). For the period search, we used 1368 counts extracted in the 0.1–2.4 keV range from a 25'' radius aperture.

Another useful observation was carried out with the *ROSAT* HRI on 1995 November 2–8 (30.7 ks useful exposure, 580 ks total time span). We evaluated the background-subtracted source count rate, 0.070 ± 0.002 s $^{-1}$ (0.080 ± 0.003 after the dead-time correction). An analysis of the radial distribution of the source counts does not show significant deviations from the HRI Point Spread Function for a point source. To reduce the background contamination, we used 1968 counts collected from a 10'' radius aperture centered at the point source ($\alpha_{2000} = 8^{\text{h}}21^{\text{m}}57^{\text{s}}.5$, $\delta_{2000} = -43^{\circ}00'14''.5$).

The *ROSAT* HRI observations of 1991 and 1992 were too short (2.4 and 1.5 ks, respectively) to collect enough point source photons. RX J0822–4300 was also observed with the *ASCA* GIS (1993 July), but a too low time resolution, 65.2 ms.

To search for periodicity of RX J0822–4300, we converted the spacecraft clock (SCC) arrival times of the HRI and PSPC photons to UTC times, and then to barycentric dynamical times (TDB). The SCC-UTC conversion was performed with a fourth order polynominal fit of the SCC calibration points to UTC. The fit residuals were within a 3 ms range; this corresponds to a scatter in pulse phase < 0.1 for frequencies $\lesssim 30$ Hz.

To perform a global periodicity search of sparse data, tests based on Z_m^2 statistics (m is the number of harmonics included) look most appropriate (Buccheri et al. 1983; De Jager 1994). Since the point source spectrum is likely of a thermal origin (PBW96; Zavlin et al. 1998b), the pulse profile is expected to be smooth, with main contributions coming from the first harmonic, as observed in thermal X-ray radiation from radio pulsars (e.g., Anderson et al. 1993) and predicted by NS atmosphere models (Shibanov et al. 1995). This means that the Z_1^2 (Rayleigh) test should

be optimal for the periodicity search: the ephemeris parameters f and \dot{f} are estimated as the values that give the largest value of $Z_1^2 = 2N^{-1}[(\sum_{i=1}^N \cos 2\pi\phi_i)^2 + (\sum_{i=1}^N \sin 2\pi\phi_i)^2]$, where N is the total number of events analyzed, $\phi_i = f\Delta t_i + \dot{f}(\Delta t_i)^2/2$ is the phase, f and \dot{f} are the trial ephemeris parameters, Δt_i ($i = 1, \dots, N$) is the event arrival time counted from an epoch of zero phase.

If the arrival times are uniformly distributed (periodic component is absent), then the probability density function of Z_1^2 is equal to that of a χ^2 with two degrees of freedom, with both the mean and the standard deviation equal to 2. The expected (mean) number of peaks with $Z_1^2 > \bar{Z}_1^2$ in \mathcal{N} statistically independent trials is $\mathcal{N} \exp(-\bar{Z}_1^2/2)$. This means that if a maximum value of Z_1^2 in an f, \dot{f} domain is such that $\alpha \equiv \mathcal{N} \exp(-Z_{1,\max}^2/2) < 1$, periodicity at the corresponding f and \dot{f} can be established at a confidence level of $C = (1 - \alpha) \times 100\%$.

For a sinusoidal signal with frequency f_0 , frequency derivative \dot{f}_0 , and pulsed fraction p , the mean and the standard deviation of the peak value $Z_1^2(f_0, \dot{f}_0)$ can be estimated as $Np^2/2$ and $(2N)^{1/2}p$, respectively, provided $Np^2 \gg 4$ and $p^2 \ll 1$. This means that the periodicity can be established at a high confidence level C only if N and p are so large, and/or \mathcal{N} so small, that $\mathcal{N} \exp(-Np^2/4) \leq 1 - (C/100\%)$. If the quantity in the left-hand side of this inequality is not small enough, the peak corresponding to the true ephemeris parameters may be comparable to, or even lower than statistical fluctuations of Z_1^2 at other values of f and \dot{f} . In this case, the true parameters f_0 and \dot{f}_0 cannot be determined reliably from a single observation.

The number \mathcal{N} of statistically independent trials is determined by the domain of f, \dot{f} values chosen for the search, and by the time span T_{span} of a given observation. If $|\dot{f}_{\max} - \dot{f}_{\min}|T_{\text{span}}^2/2 \ll 1$, then Z_1^2 is almost independent of \dot{f} , and one can use a one-dimensional (frequency) grid at a fixed \dot{f} from the range chosen. The number of independent trials is $\mathcal{N} = (f_{\max} - f_{\min})T_{\text{span}}$, and the number of grid points should be greater by a factor of ~ 10 , in order not to miss the peak. In the opposite case, $|\dot{f}_{\max} - \dot{f}_{\min}|T_{\text{span}}^2/2 \gtrsim 1$, one has to use a two-dimensional f, \dot{f} grid, with $\mathcal{N} = (f_{\max} - f_{\min})|\dot{f}_{\max} - \dot{f}_{\min}|T_{\text{span}}^3/2$ and the number of the grid points of $\sim 10^2\mathcal{N}$.

A reasonable f, \dot{f} domain for a young, isolated NS is $0.01 \lesssim f \lesssim 100$ Hz, $-1 \times 10^{-10} \lesssim \dot{f} \leq 0$ Hz s $^{-1}$. The 3 ms accuracy of the SCC-UTC conversion hampers detection of high-frequency modulation, so that we choose a conservative upper limit, $f \leq 30$ Hz. For the f, \dot{f} domain chosen, Z_1^2 is practically independent of \dot{f} for the PSPC observation ($|\dot{f}|_{\max}T_{\text{span}}^2/2 = 0.14$), contrary to the HRI observation ($|\dot{f}|_{\max}T_{\text{span}}^2/2 = 17$), and the numbers of independent trials are $\mathcal{N} = 1.6 \times 10^6$ and 2.9×10^8 , respectively. Because of the enormous number of the two-dimensional grid points needed for the blind periodicity search in the HRI data, we have to start from investigating Z_1^2 for the PSPC events, the first step of our timing analysis. We put $\dot{f} = 0$ and calculated $Z_1^2(f)$ at equally spaced 2×10^7 frequencies in the range 0.01–30 Hz. The result is not encouraging — the highest peak, $Z_1^2 = 32.0$, is not much higher than several other peaks ($Z_1^2 = 30.5, 29.8, 29.1, 27.8$), and the probability that $Z_1^2 > 32$ for uniformly distributed arrival times is as large as 0.18. Although any one of these peaks could be caused by

real pulsations, with an expected pulsed fraction $p = 20.9(Z_1^2/30)^{1/2}\%$ for a sine-like pulse profile, the corresponding confidence level would be too low (e.g., 82%, or 1.3σ , for $Z_1^2 = 32$) to claim the periodicity is detected. Thus, we have to conclude that only an upper limit on the pulsed fraction, $\approx 20\%$, can be established from the PSPC data alone, in accordance with PBW96.

However, with one more set of timing data available, we can examine whether the separate PSPC Z_1^2 peaks correspond to HRI Z_1^2 peaks at reasonably shifted frequencies. If a PSPC peak at $f = f_{\text{PSPC}}$ is caused by a periodic signal, then Z_1^2 calculated with the HRI arrival times should have a peak at a frequency $f_{\text{HRI}} = f_{\text{PSPC}} + \dot{f}T$, where $T = 1661^d 00003469$ is the time in the TDB scale between the epochs (start times) of the PSPC and HRI observations. If such a peak is not found for reasonable values of \dot{f} , we have to conclude that the PSPC peak under examination is most likely a statistical fluctuation. Thus, the second step of our analysis is a conditional search for periodicity in narrow strips of the f_{HRI}, \dot{f} plane. The width of the strip along the f_{HRI} axis, $\Delta f_{\text{HRI}} = 2/T_{\text{span}}^{\text{PSPC}} \simeq 4 \times 10^{-5}$ Hz, is determined by the uncertainty of f_{PSPC} due to the finiteness of the time span. The size of the strip along the \dot{f} axis is merely $|\dot{f}|_{\text{max}} = 1 \times 10^{-10}$ Hz s $^{-1}$. The number of statistically independent trials for each of the strips can be estimated as $\mathcal{N} = \Delta f_{\text{HRI}} |\dot{f}|_{\text{max}} (T_{\text{span}}^{\text{HRI}})^3 / 2 \simeq 370$.

We examined the ten highest PSPC peaks and found no corresponding HRI peaks of a high significance for nine of them — heights of the HRI peaks do not exceed $Z_1^2 = 16.5$, which corresponds to confidence levels $C < 90.4\%$ ($< 1.7\sigma$). Only for one PSPC peak, $Z_1^2 = 30.5$ at $f_{\text{PSPC}} = 13.2875651(8)$ Hz, a highly significant ($C > 99.95\%$, or $> 3.5\sigma$) HRI counterpart was found, $Z_1^2 = 27.3$ at $f_{\text{HRI}} = 13.28378836(7)$ Hz and $\dot{f} = -2.63(2) \times 10^{-11}$ Hz s $^{-1}$. The digits in parentheses indicate uncertainties, q/T_{span} and $2q/T_{\text{span}}^2$, of the last digits of f and \dot{f} , where $q \simeq (3 \text{ ms}) f_0 \simeq 0.04$ is a phase resolution (cf. Mattox et al. 1996). The values of the PSPC and HRI ephemeris parameters are for the (TDB) epochs MJD 48361 $^d 50067344$ and MJD 50022 $^d 50070813$, respectively. The period and its derivative, for the latter epoch, are $P = 75.2797300(4)$ ms, $\dot{P} = 1.49(1) \times 10^{-13}$ s s $^{-1}$. To verify that the PSPC and HRI Z_1^2 peaks are indeed associated with RX J0822–4300, we applied the Z_1^2 test to comparable numbers of off-source events in the PSPC and HRI observations and obtained Z_1^2 values close to the mean value expected for a nonpulsed signal. Figure 1 shows the frequency dependences $Z_1^2(f)$ at fixed $\dot{f} = \dot{f}_0$ for the PSPC and HRI data. The main (highest) peaks at $f = f_0$ are accompanied by a few side peaks at $f = f_0 \pm 1.74 \times 10^{-4}k$ Hz ($k = 1, 2, \dots$), caused by exposure gaps associated with the *ROSAT* revolution around Earth with the period of 96.0 min. Both the main and the side peaks have an additional fine structure with characteristic “periods” $1/T_{\text{span}}^{\text{PSPC}} = 1.9 \times 10^{-5}$ Hz and $1/T_{\text{span}}^{\text{HRI}} = 1.7 \times 10^{-6}$ Hz. Similar coherent structures can be also seen in the dependence of the HRI Z_1^2 on \dot{f} at a fixed f , with a shortest “period” $2/(T_{\text{span}}^{\text{HRI}})^2 = 5.9 \times 10^{-12}$ Hz s $^{-1}$.

Figure 2 shows the pulse profiles extracted by folding the arrival times with the ephemeris parameters obtained for the PSPC and HRI data sets. Each of the curves is drawn for the corresponding epoch, which causes the apparent phase shift. This shift could be eliminated by combining the PSPC and HRI events in one set and determining the ephemeris parameters with a

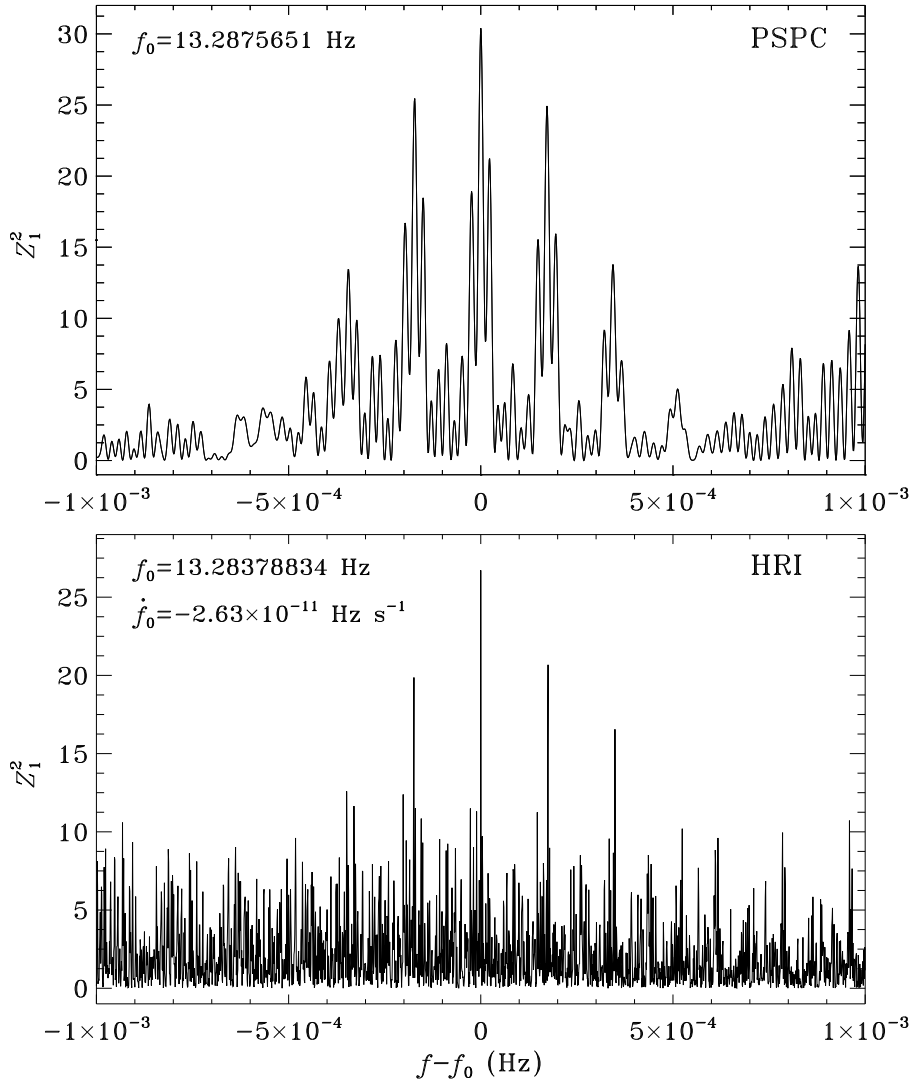


Fig. 1.— Power spectra around the pulsar frequency f_0 for the PSPC (1991 April) and HRI (1995 November) observations, at the frequency derivative $\dot{f} = -2.63 \times 10^{-11} \text{ Hz s}^{-1}$.

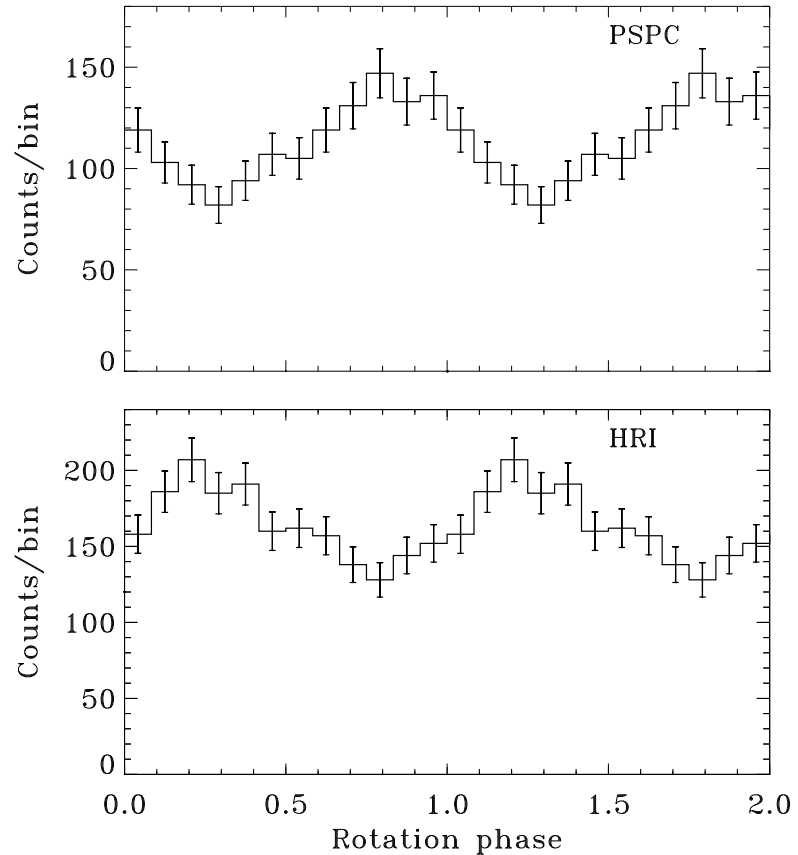


Fig. 2.— Folded light curves for the PSPC and HRI data.

much higher accuracy, but the total time span, $T_{\text{span}} \simeq 1.441 \times 10^8$ s, is so long that this cannot be done unequivocally. We verified that there is no statistically significant difference between the shapes of the PSPC and HRI pulses. The light curves binned in 12 phase bins have broad maxima consistent with a thermal origin of the X-ray flux. The powers of higher harmonics are small in comparison with Z_1^2 (3.2 vs. 30.5 and 1.0 vs. 27.3), which demonstrates the pulse profile shape is close to a sinusoid and justifies *a posteriori* our choice of Z_1^2 as a test statistic. To estimate the pulsed fractions, we applied the bootstrap method proposed by Swanepoel, de Beer & Loots (1996) and obtained $p = 22.5 \pm 4.2\%$ and $20.1 \pm 3.5\%$ for the PSPC and HRI light curves, respectively. We also calculated the PSPC pulse profiles at lower and higher photon energies (0.1–1.1 and 1.1–2.4 keV) and found no statistically significant phase shift or difference of the pulse shapes.

3. Discussion

With the period and its derivative evaluated, it is straightforward to estimate the pulsar's age, magnetic field, and rotational energy loss. Assuming a pulsar spin-down equation $\dot{f} = -Kf^n$, where n is the braking index and $K = \text{const}$, the characteristic (dynamical) pulsar's age equals $\tau = -f/[(n-1)\dot{f}] = 16.0/(n-1)$ kyr, provided that the rotational rate at the NS birth was much greater than its current value, $f_{\text{in}} \gg f$. For $n = 3$, corresponding to a simple magnetic-dipole braking, we obtain $\tau = 8.0$ kyr. If we accept that the true pulsar age coincides with the the kinematic age of the SNR, 3.7 ± 0.4 kyr, then the braking index should be $n = 5.3 \pm 0.5$. To match the pulsar's age and the kinematic SNR age at $2.2 < n < 2.9$, observed for the youngest radio pulsars PSR B0531+21, B0540–69, B1509–58, f_{in} should be within a 16.8–18.9 Hz range ($P_{\text{in}} = 53\text{--}59$ ms). A remarkably similar situation with the SNR/pulsar age and the braking index is found for PSR J1617–5055 near the SNR RCW 103 (Torii et al. 1998; Kaspi et al. 1998). The conventional “magnetic field” of the pulsar, derived from the standard formula $B = 1.0 \times 10^{12}(P\dot{P}_{-15})^{1/2}$ G (e. g., Manchester & Taylor 1977), equals 3.4×10^{12} G for a standard moment of inertia, $I = 10^{45}$ g cm², and a NS radius of 10 km. The rotational energy loss can be estimated as $\dot{E} = -4\pi^2 I \dot{f} f = 1.4 \times 10^{37}$ erg s^{−1}. The parameters inferred for RX J0822–4300 are close to those of the Vela pulsar, $P = 89.3$ ms, $\dot{P} = 1.25 \times 10^{-13}$, $P/(2\dot{P}) = 11$ kyr, $B = 3.4 \times 10^{12}$ G, $\dot{E} = 0.7 \times 10^{37}$ erg s^{−1}.

These results indicate that RX J0822–4300 may be a regular radio pulsar whose radio-quiet nature can be explained by an unfavorable orientation of the pulsar beam. Contrary to the radio flux, the X-rays observed from RX J0822–4300 originate from the whole NS surface (Zavlin et al. 1998b), their pulsation with $p \simeq 20\%$ may be due to anisotropy of the surface temperature distribution and magnetized atmosphere radiation. However, it is expected that the lower is the frequency, the broader is the radio beam. Therefore, deep radio observations at low frequencies could detect RX J0822–4300, as it has happened recently with Geminga (Kuzmin & Losovsky 1997; Malofeev & Malov 1997).

Such a young, energetic pulsar is expected to power a pulsar wind nebula, either in the form

of a plerion or a bow shock. The *ROSAT* images show two “blobs”, $\approx 2'$ north and $\approx 1'$ south of the NS, with luminosities $L_x \sim (1 - 2) \times 10^{34} d_2^2$ erg s $^{-1}$ in the *ROSAT* range; the blobs are apparently connected to the NS with strips of lower brightness. In addition, the *ASCA* GIS image at higher energies, $E > 3$ keV, reveals a structure resembling a bow-shock nebula, about $5' - 6'$ east of RX J0822–4300. Although these structures might be manifestations of the pulsar activity, one still cannot firmly exclude that they belong to the SNR and are not physically associated with the pulsar. Future X-ray and radio observations of RX J0822–4300 and its environment are needed to elucidate the nature of these structures.

It is our pleasure to thank Rob Petre, the referee, for very valuable comments. The data preparation for the timing analysis was done with the *EXSAS* software developed at MPE. This work was partially supported through NASA grants NAG5-6907 and NAG5-7017.

REFERENCES

Anderson, S. B., Cordova, F. A., Pavlov, G. G., Robinson, C. R., & Thomson, R. J. 1993, *ApJ*, 414, 867

Brazier, K. T.S., & Johnston, S. 1998, *MNRAS*, submitted

Buccheri, R., et. al. 1983, *A&A*, 128, 245

De Jager, C. O. 1994, *ApJ*, 436, 239

Greenstein, G., & Hartke, G. J. 1983, *ApJ*, 271, 283

Kaspi, V. M., et al. 1998, *ApJ*, 503, L161

Kuzmin, A. D., & Losovsky, B. Y. 1997, *Astron. Let.*, 23, 323

Malofeev, V. M., Malov O. I. 1997, *Nature*, 389, 697

Manchester, R. N., & Taylor, J. H. 1977, *Pulsars* (San Francisco: Freeman)

Mattox, J. R., Halpern, J. P., & Caraveo, P. A. 1996, *A&AS*, 120, 77

Petre, R., Canizares, C. R., Kriss, G. A., & Winkler, P. F. 1982, *ApJ*, 440, 706

Petre, R., Becker, C. M., & Winkler, P. F. 1996, 465, L43 (PBW96)

Reynoso, E. M., Dubner, G. M., Goss, W. M., & Arnal, E. M. 1995, *AJ*, 110, 318

Shibanov, Yu. A., Pavlov. G. G., Zavlin, V. E., Qin, L., & Tsuruta, S. 1995, in *The 17th Texas Symposium on Relativistic Astrophysics and Cosmology*, eds. H. Böhringer, G. E. Morfill & J. E. Trümper (NY: NY Academy of Science), 759, p. 291

Swanepoel, J. W. H., de Beer, C. F., Loots, H. 1996, *ApJ*, 467, 261

Torii, K., et al. 1998, *ApJ*, 494, L207

Vasisht, G., & Gotthelf, E. F. 1997, *ApJ*, 486, L29

Winkler, P. F., Tuttle, J. H., Kirshner, R. P., & Irwin, M. J. 1988, in Supernova Remnants and the Interstellar Medium, eds. R. S. Roger & T. L. Landecker (Cambridge: Cambridge Univ. Press), p. 65

Zavlin, V. E., Pavlov, G. G., & Trümper, J. 1998a, A&A, 331, 821

Zavlin, V. E., Pavlov, G. G., & Trümper, J. 1998b, ApJ, in preparation